catalysts

MDPI

Article

Iron-Borophosphate Glass-Catalyzed Regioselective Hydrothiolation of Alkynes under Green Conditions

Nicoli Catholico [1], Eduarda A. Tessari [2], Isis J. A. Granja [3], Martinho J. A. de Sousa [4], Jorlandio F. Felix [5], Flávia Manarin [2], Marcelo Godoi [6], Jamal Rafique [3,4], Ricardo Schneider [7,*], Sumbal Saba [3,*] and Giancarlo V. Botteselle [1,*]

1 Department of Chemistry, Midwestern Parana State University-UNICENTRO, Guarapuava 85040-167, PR, Brazil; nicolicatholico@yahoo.com.br
2 Center for Engineering and Exact Sciences, Western Parana State University-UNIOESTE, Toledo 85903-000, PR, Brazil; eduardatessari@hotmail.com (E.A.T.); fgmanarin@gmail.com (F.M.)
3 Instituto de Química IQ, Universidade Federal de Goiás-UFG, Goiania 74690-900, GO, Brazil; isisgranja@gmail.com (I.J.A.G.); jamal.chm@gmail.com or jamal.rafique@ufms.br (J.R.)
4 Institute of Chemistry-INQUI, Federal University of Mato Grosso do Sul-UFMS, Campo Grande 79074-460, MS, Brazil; martinhotinho@hotmail.com
5 Institute of Physics, University of Brasilia-UNB, Brasilia 70910-900, DF, Brazil; jorlandio@unb.br
6 School of Chemistry and Food, Federal University of Rio Grande-FURG, Santo Antanio da Patrulha 95500-000, RS, Brazil; marcelogodoi@furg.br
7 Group of Polymers and Nanostructures, Federal University of Technology Parana-UTFPR, Toledo 85902-490, PR, Brazil
* Correspondence: rschneider@utfpr.edu.br (R.S.); sumbalsaba@ufg.br (S.S.); giancarlo@unicentro.br (G.V.B.)

Abstract: Vinyl sulfides are an important class of organic compounds that have relevant synthetic and biological applications. The best-known approach to realize these compounds is the hydrothiolation of alkynes under different conditions using metals, toxic and carcinogenic solvents. The development of new catalysts using materials that are environmentally friendly, low in cost, and easy to handle is highly desirable for this reaction. In this regard, glasses have become an important class of materials, since they can be used as a catalyst for chemical reactions. We prepared and characterized an inexpensive and robust iron-doped borophosphate glass (Fe@NaH_2PO_4-H_3BO_3 glass). This eco-friendly material was successfully applied as a catalyst for the hydrothiolation of alkynes under solvent-free conditions, affording the desired vinyl sulfides in good-to-excellent yields, with high stereoselectivity. This method of synthesis is attractive because it enables the reuse of the iron-glass catalyst and the scaling up of reactions.

Keywords: iron-borophosphate glass; catalysis; vinyl sulfides; hydrothiolation; green chemistry

Citation: Catholico, N.; Tessari, E.A.; Granja, I.J.A.; de Sousa, M.J.A.; Felix, J.F.; Manarin, F.; Godoi, M.; Rafique, J.; Schneider, R.; Saba, S.; et al. Iron-Borophosphate Glass-Catalyzed Regioselective Hydrothiolation of Alkynes under Green Conditions. *Catalysts* **2023**, *13*, 1127. https://doi.org/10.3390/catal13071127

Academic Editors: Victorio Cadierno and Raffaella Mancuso

Received: 23 June 2023
Revised: 18 July 2023
Accepted: 18 July 2023
Published: 20 July 2023

1. Introduction

Glasses or glass-based materials are known for their stability and the high temperature commonly required for their synthesis. While glasses can be made using different approaches, the melting and fast-cooling method is widely used. Phosphates, and to some extent phosphate-based glasses, are a distinct group of materials that can be obtained from simple and eco-friendly raw chemicals. However, they usually have low chemical stability (e.g., high moisture sensitivity). Nevertheless, their ability to dissolve oxides at relatively low temperature overcomes the lability of the phosphate network [1,2]. Not only is the modification of the glass network achieved by addition of modifiers (dissolved ions) but also the reactivity of the glass surface [3]. Using appropriate oxides and/or metallic oxides will produce a glass that can be handled under ordinary conditions with superior catalyst performance. In this context, iron oxide is an abundant and affordable raw chemical that can be used in the synthesis of important classes of molecules, such as organosulfur [4,5] and organoselenium compounds [6,7].

Vinyl sulfides have emerged as a well-recognized class of organosulfur compounds, and can be used in various syntheses (e.g., as a key intermediate in the total synthesis of biologically active compounds) [8–10]. Due to the applicability of organosulfur compounds, a wide range of approaches for the preparation of vinyl sulfides has been reported [11–14].

The hydrothiolation of terminal alkynes (alkyne in which the carbon–carbon triple bond is at the end of the carbon chain) has become the most eco-friendly method because it produces vinyl sulfides with high atom efficiency, as well as high levels of chemo- and stereoselectivity [15,16]. Anti-Markovnikov addition products have been successfully synthesized in high yields in the presence of different catalysts and/or reaction promoters [17,18], including sulfamic acid [19], cesium carbonate [20], and potassium phosphate [21]. The water extract of straw ash has also been used as a suitable reaction medium for the hydrothiolation reaction [22,23].

However, the most applicable and widely explored methods [24–26] employ metals such as copper [27,28], iron [29], indium [30], rhodium [31], and ruthenium [32] as catalysts. Despite the high efficiency of these approaches, the development of environmentally friendly catalysts for the hydrothiolation reaction remains a great challenge. To our knowledge, the application of iron-glass catalysts in organosulfur chemistry has not yet been explored.

In addition, solvent-free reactions are attractive alternatives in organic synthesis and are considered an important contribution to the evolution of green chemistry [33,34]. Based on our interest in developing new sustainable materials and eco-friendly processes for organic reactions and material sciences [35–40], we describe herein the synthesis of a cheap and readily available iron-borophosphate glass and its application as a recyclable catalyst for the synthesis of vinyl sulfides. This novel approach worked smoothly under solvent-free conditions in a significantly short reaction time.

2. Results and Discussion

2.1. Iron-Borophosphate Glass Characterization

Figure 1 shows the powder X-ray diffraction (PXRD) analysis of the undoped borophosphate glass ((a) in Figure 1), borophosphate glass doped with trivalent aluminum ions (Al^{3+}) ((b) in Figure 1), and borophosphate glass doped with aluminum and iron ions ((c) in Figure 1).

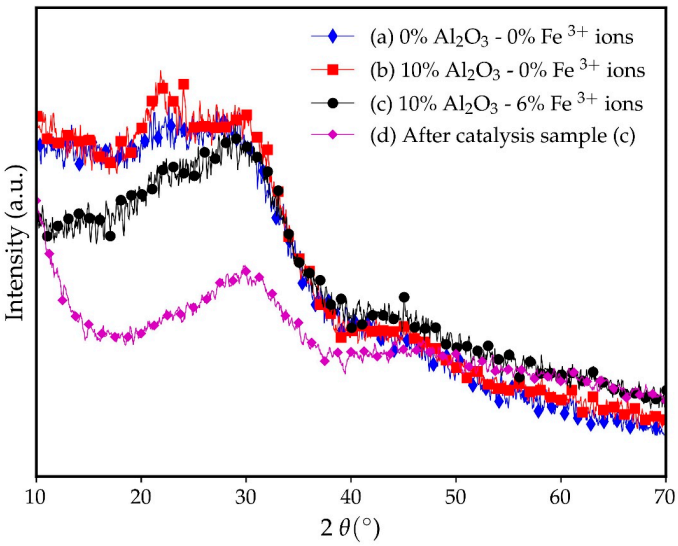

Figure 1. Powder PXRD analysis for borophosphate glass with (mol) (a) 0% Al_2O_3 and 0% Fe^{3+} ions, (b) 10% Al_2O_3 and 0% Fe^{3+} ions, and (c) 10% Al_2O_3 and 6% Fe^{3+} ions and (d) sample (c) after catalysis.

The diffractograms for all glasses show the characteristic halo of amorphous materials. Pure phosphate-based glasses suffer from moisture attack under normal conditions. Their

chemical resistance can be improved by adding transition elements and/or trivalent ions, e.g., aluminum ions. A modification with aluminum and iron ions resulted in the formation of an amorphous material within the compositional range evaluated.

Figure 2 shows the Raman spectra of the borophosphate glasses. All the spectra show broad bands in the 1340–850 cm^{-1} and 810–430 cm^{-1} regions. These broad bands correspond to an overlapping phosphate network, and the deconvoluted spectra over a range of Voigt line shapes are shown in Figure S1 (Supplementary Material). Figure S1A shows the deconvoluted Raman spectrum of the undoped borophosphate glass (without aluminum or iron ions). The peak at 1256 cm^{-1} is attributed to the antisymmetric stretching mode ν_{as} (PO_2^-) of the Q^2 units [41,42]. The peaks at 1127 cm^{-1} and 1069 cm^{-1} show the greatest overlap. The peak at 1127 cm^{-1} corresponds to the vibrations of the $P\text{Ø}_2O_2^-$ (Ø = bridging oxygen atom) tetrahedra in the Q^2 units, whereas the peak at 1069 cm^{-1} is associated with the P–O^- vibrations of pyrophosphate (Q^1 in a dimeric pyrophosphate unit, $P_2O_7^{4-}$) and/or $(PO_2)_{sym}$ in the Q^1 structure [43–45]. The shoulder at 926 cm^{-1} (Figure S1A) is a characteristic of orthophosphate (Q^0) units, i.e., the symmetric stretching mode (ν_s) of P−O^- non-bridging oxygen bonds in the PO_4^{3-} tetrahedra [43,45]. In the phosphate glasses, the band at 700 cm^{-1} is associated with P−O−P stretching. The band splits into two distinct bands upon the addition of boron to the glass matrix [45]. The two shoulders at 768 cm^{-1} and 726 cm^{-1} are attributed to the P–O–P vibrations and the presence of boron atoms in the glass network, respectively. Anastasopoulou et al. [43] assigned the shoulder at 768 cm^{-1} (the dashed line in Figure 2) to the symmetric stretching (ν_s (P−O−P)) of the phosphate or borophosphate chains. The shoulder at 726 cm^{-1} (solid line in Figure 2) is tentatively attributed to the presence of borophosphate rings. The band at 343 cm^{-1} is assigned to the bending mode of the phosphate network [46].

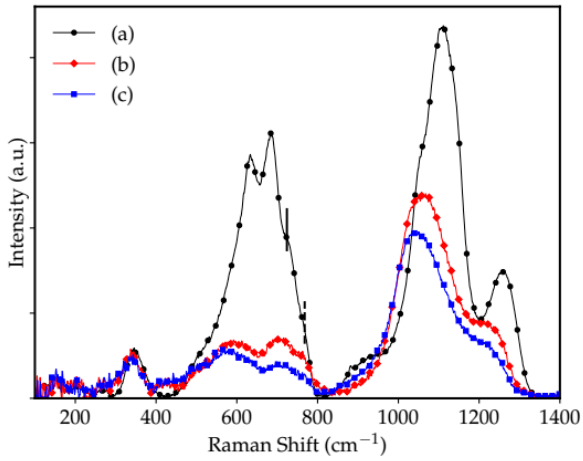

Figure 2. Raman spectrum for borophosphate glass (in mol%) (a) 0% Al_2O_3 and 0% Fe^{3+} ions, (b) 10% Al_2O_3 and 0% Fe^{3+} ions, and (c) 10% Al_2O_3 and 6% Fe^{3+} ions.

The glass structure was considerably changed after the addition of aluminum ions (Figure S1B). Both aluminum ions and iron ions caused the phosphate network to depolymerize. Moguš-Milanković et al. [44] suggested that iron ions can depolymerize the P–O–P and P–O–Al bonds. The addition of aluminum shifted the main bands to lower wavenumbers. The deconvolution of the Q^1 and Q^2 overlap in the 1340–850 cm^{-1} region of the Al-doped borophosphate glass showed peaks at 928 cm^{-1}, 1043 cm^{-1}, 1108 cm^{-1}, 1180 cm^{-1}, and 1244 cm^{-1}.

The shoulder at 928 cm^{-1} remains associated with the Q^0 units, as discussed previously. After the addition of aluminum, the peak at 1069 cm^{-1}, which is associated with the P–O^- vibrations of pyrophosphate, increased in intensity and was displaced to 1043 cm^{-1} (Figure S1B) [43–45]. This increase in intensity is associated with the replacement of P−O−P bonds by P−O−Al bonds. The peak at 1108 cm^{-1}, related to the vibrations of the $P\text{Ø}_2O_2^-$ tetrahedra in the Q^2 units and originally the most intense at 1127 cm^{-1} in

the undoped sample, decreased in intensity due to depolymerization of the glass network. The peaks at 1180 cm^{-1} and 1244 cm^{-1} are assigned to ν_s (PO_2) and ν_{as} (PO_2) of the non-bridging oxygen bonds in the Q^2 units, respectively [44]. In turn, the addition of iron ions to the glass matrix reduced the intensity of the main bands and shifted them to slightly lower wavenumbers (Figure S1C). The deconvoluted spectrum of the iron-doped borophosphate glass showed peaks at 919 cm^{-1}, 1035 cm^{-1}, 1104 cm^{-1}, 1176 cm^{-1}, and 1239 cm^{-1}. The peak at 1035 cm^{-1}, associated with the Q^1 units, dominated the 1340–850 cm^{-1} region. Moreover, the intensities of the peaks related to the Q^2 units at 1104 cm^{-1}, 1176 cm^{-1}, and 1239 cm^{-1} were reduced. For example, the shoulder on the right side of the main band, which consists of peaks at 1176 cm^{-1} and 1239 cm^{-1}, became less intense with the addition of iron. From this, we can infer that at this concentration, the addition of iron depolymerizes the glass instead of replacing the P−O−Al bonds.

2.2. Regioselective Hydrothiolation of Alkynes

To determine the applicability of iron-borophosphate glass (Fe@NaH_2PO_4-H_3BO_3 glass), it was tested as a catalyst in the regioselective hydrothiolation of alkynes. We first conducted studies to determine the optimal synthesis conditions. For this purpose, methylbenzenethiol (**1a**) and phenylacetylene (**2a**) were used as the model substrates under solvent-free conditions. The catalytic potential of Fe@NaH_2PO_4-H_3BO_3 glass was then screened under various reaction conditions (Table 1).

Table 1. Determination of reaction conditions [a].

Entry	Catalyst Amount (mg)	Time (min)	Temp (°C)	Yield (%) [b]	*E*:*Z* [c]
1	Fe@NaH_2PO_4-H_3BO_3 (10)	10	r.t.	80	60:40
2	Fe@NaH_2PO_4-H_3BO_3 (10)	10	0	80	75:25
3	Fe@NaH_2PO_4-H_3BO_3 (10)	10	−5	39	82:18
4	Fe@NaH_2PO_4-H_3BO_3 (10)	10	50	61	81:19
5	Fe@NaH_2PO_4-H_3BO_3 (5)	10	0	65	90:10
6	Fe@NaH_2PO_4-H_3BO_3 (15)	10	0	60	60:40
7	Fe@NaH_2PO_4-H_3BO_3 (10)	20	0	55	75:25
8	Fe@NaH_2PO_4-H_3BO_3 (10)	30	0	60	76:24
9	Fe@NaH_2PO_4-H_3BO_3 (10)	40	0	97	82:18
10	Fe@NaH_2PO_4-H_3BO_3 (10)	40	r.t.	66	75:25
11	Fe@NaH_2PO_4-H_3BO_3 (10)	40	−5	44	88:12
12	NaH_2PO_4-H_3BO_3 (10)	40	0	77	77:23
13 [d]	Fe_2O_3	40	0	59	89:11
14	-	10	0	-	-

[a] Reaction conditions: 4-methylbenzenethiol **1a** (0.25 mmol), phenylacetylene **2a** (0.25 mmol) and glass catalyst; [b] isolated yield; [c] stereoisomers were determined by ^{1}H NMR spectroscopy; [d] 5.0 mol% was used as catalyst, which is approximately the amount of iron oxide in the glass matrix.

Firstly, the optimal temperature for the hydrothiolation reaction was evaluated using catalytic amounts of Fe@NaH_2PO_4-H_3BO_3 glass (10 mg). At 0 °C, the desired product **3a** was synthesized in a good yield, with high stereoselectivity (entries 1−4). Next, we evaluated the catalyst loading for the reaction. When the amount of the catalyst was decreased to 5 mg, the stereoselectivity was high (*E*/*Z* ratio = 90:10), but the yield of **3a** was only 65% (entry 5). In the same way, when the loading of catalyst was increased to 15 mg, **3a** was synthesized in 60% yield, with very poor stereoselectivity (entry 6). As such, 10 mg (approximately 4.3 mol % of Fe_2O_3) was the most appropriate catalyst load for this reaction, where the desired product was synthesized in 80% yield and with high stereoselectivity (entry 2).

After determining the best temperature and catalyst load, we evaluated the influence of the reaction time (entries 7–9). We found that 40 min was the best reaction time, where **3a** was synthesized in 97% yield, with an *E*/*Z* ratio of 82:18 (entry 9). In addition, no improvement in yield or stereoselectivity was observed when the reaction was carried out in different temperatures for 40 min (entries 10–11).

Finally, to determine the efficiency of Fe@NaH_2PO_4-H_3BO_3 glass in the hydrothiolation reaction, we independently investigated the influence of the metal and pure borophosphate glass (NaH_2PO_4-H_3BO_3) on the reaction. When the reaction was carried out using pure NaH_2PO_4-H_3BO_3, **3a** was obtained in a lower yield, with lower stereoselectivity

(entry 12). Similarly, a low yield of product **3a** was observed when commercial Fe_2O_3 was used (entry 13). No product was observed when the reaction was performed without the catalyst (entry 14). These results highlight that the presence of iron in the glass matrix affects the reaction and allows for the product to be synthesized in high yields with high stereoselectivity.

After determining the best reaction conditions (Table 1, entry 9), the synthesis method was extended to other thiols (**1**) and acetylenes (**2**) to evaluate its generality and scope (Figure 3). In general, the aromatic thiols reacted very smoothly with phenylacetylene, affording the desired products in 65–97% yields (Figure 3, **3a**–**e**). In terms of selectivity, the aryl groups attached to the sulfur moiety played a significant role in the resulting stereochemistry of the products. Large amounts of *E* stereoisomer were obtained for compounds **3a**–**d**. For example, the reaction of thiophenol **2b** with phenylacetylene **1a** delivered the compound **3b** in 82% yield and stereoselectivity of *E*/*Z* ratio = 67:33. It is important to note that sulfide **3c**, which is synthesized from 4-chlorothiophenol, was obtained in 76% yield exclusively in the *E* configuration. When the bromo atom was attached in a *para* position of the aromatic ring of thiol, the desired product **3d** was obtained in 65% yield with an *E*/*Z* ratio of 70:30.

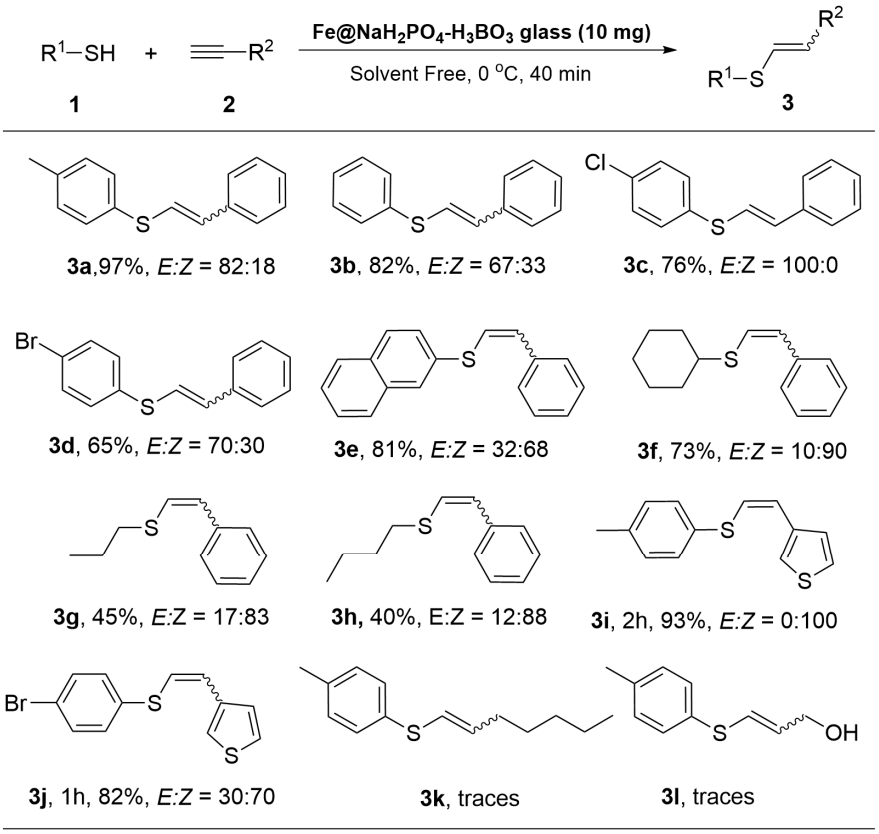

Figure 3. Synthesis of vinyl sulfides catalyzed by iron-borophosphate glass. Reaction conditions: thiol (0.25 mmol), acetylene (0.25 mmol) and Fe@NaH_2PO_4-H_3BO_3 (10 mg). Isolation of products using column chromatography and stereoisomers determined by ^{1}H NMR spectroscopy.

For sulfur moieties containing naphthyl and alkyl groups, however, the *Z* stereoisomer of the vinyl sulfides was preferred. For example, when 2-naphthalene thiol was employed, **3e** was obtained in 81% yield, with an *E*/*Z* ratio of 32:68. The cyclohexyl vinyl sulfide derivative **3e** was obtained in 73% yield, with high stereoselectivity (*E*/*Z* ratio = 10:90). Although a relatively low yield was obtained when thiol derivatives containing propyl and butyl groups were used, the stereoselectivity of **3g** and **3h** remained high.

The method was also found to be applicable to the hydrothiolation of 3-ethynylthioph ene, where the products **3i** and **3j** were synthesized in excellent yields (93% and 82%,

respectively), with high *Z* stereoselectivity. In particular, **3i** was obtained in 100% of its *Z* stereoisomer. The method, however, was not applicable for the hydrothiolation of 1-heptyne and propargyl alcohol, as seen from the trace amounts of products **3k** and **3l** produced under similar reaction conditions.

In order to demonstrate the synthetic utility of this protocol, scaling up of the reaction was performed at 5.0 mmol (Figure 4). In this experiment, 4-methylbenzenethiol **1a** and phenylacetylene **2a** were used as the starting materials, affording the vinyl sulfide **3a** with excellent yield: 97% (1.10 g). Thus, this methodology could be used for gram-scale synthesis of vinyl sulfides.

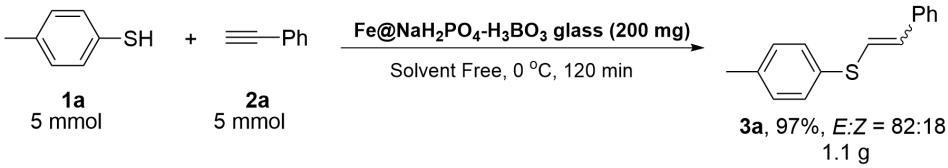

Figure 4. Scaling up reaction for the synthesis of 1.1 g of compound **3a**.

To further evaluate the efficacy of the catalyst (Fe@NaH_2PO_4-H_3BO_3 glass) for the subsequent catalytic cycle, a standard reaction was performed (Table 1, entry 9). After the reaction, the catalysts were recovered from the reaction medium by adding EtOAc (3 × 5.0 mL) and the organic phase was removed by using a Pasteur pipette. The recovered catalysts were dried in ambient atmosphere and used directly in other reactions without any purification. The recycled iron-glass catalyst was reused for more four reaction cycles, coupling **1a** and **2a**. To our delight, the catalyst maintained its effectiveness, yielding **3a** without significant decrease in the yields (Figure 5). Furthermore, we performed PXRD ((d) in Figure 1) and Raman (Figure S1D) measurements of the glass-based catalyst after catalysis. The glass-based catalyst after the catalytic run retained its amorphous character. The Raman spectra show a profile similar to the glass structure.

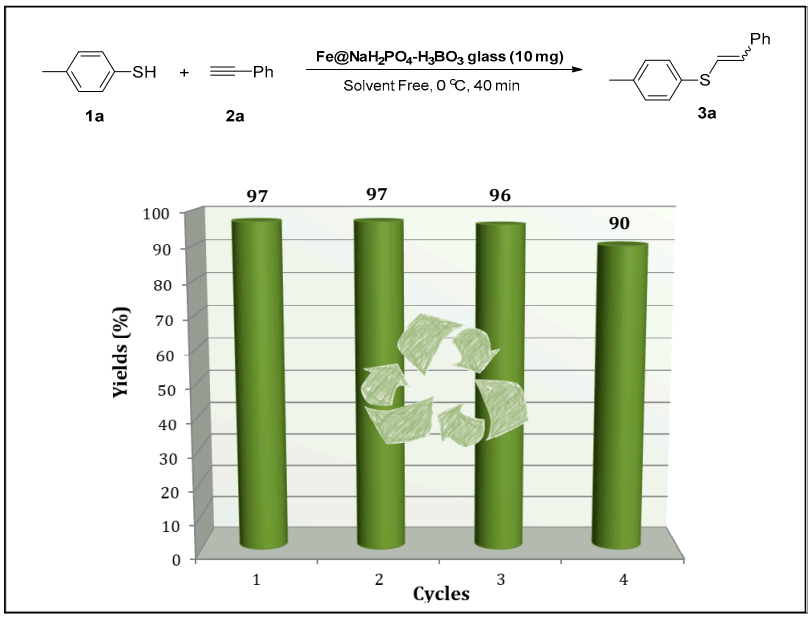

Figure 5. Recyclability of the catalyst.

3. Materials and Methods

3.1. General Information

The reagents and solvents were purchased commercially from Sigma-Aldrich-Merck and LabSynth. The organic reactions were monitored by thin-layer chromatography (TLC). The TLC plates were observed under UV light and iodine vapor. The nuclear resonance

spectroscopy (NMR) spectra were obtained on a Bruker DPX-300 Avance spectrometer, using deuterated chloroform ($CDCl_3$) as solvent. The structural information of the glass matrix was accessed by Raman spectroscopy. The spectra were obtained in powdered samples (325 mesh) using a 514.5 nm excitation source in a LabRAM HR Evolution System from Horiba. The spectra were collected in the 100–1400 cm^{-1} range using a CCD camera at room temperature. The powder X-ray diffraction (PXDR) analyses of the glasses were performed using a glass plate holder. The borophosphate glass powder was gently mounted on the glass holder. The diffractograms of the powder were obtained using Bragg–Brentano (BB) geometry in a SmartLab SE 3 kW diffractometer from Rigaku equipped with Cu-Kα radiation source (λ = 1.5418 Å) in the 15–80 θ–2θ (°) range.

3.2. Glass Synthesis

The borophosphate glass matrix was composed of NaH_2PO_4 and H_3BO_3 with NaH_2PO_4/H_3BO_3 (mol) ratio of 2, modified with 10 mol% of Al_2O_3, and doped with iron ions from Fe_2O_3 addition at 3 mol%.

Usually, a 30 mL Pt/Au (95%/5%) crucible with a lid is used to run 10 g batches of the raw chemicals previously homogenized for ten minutes in an agate mortar. The glass raw chemicals were fused in a preheated resistive furnace at 1050 °C for 60 min.

After that, the glass melts were quenched to room in a cylindrical graphite mold. The glass-based catalyst powder was obtained by crushing the pieces and sieving them through a 325-mesh sieve.

3.3. General Procedure for the Preparation of Vinyl Sulfides

To a test tube contain a stirring bar was added 10 mg of iron-borophosphate glass (catalyst) and placed in an ice bath at 0 °C. After that, the respective acetylene (0.25 mmol) was added and subsequently the thiol (0.25 mmol), followed by stirring for 40 min at 0 °C. The hydrothiolation reaction was monitored by thin-layer chromatography (TLC) using hexane as eluent to determine reaction time. The organic compounds were solubilized in ethyl acetate (3 × 5.0 mL), separated by filtration, and concentrated under vacuum. The purification of the products was carried out by column chromatography, using silica gel (silica gel 60, 0.005–0.10 mm) as stationary phase and hexane as mobile phase. The identity, purity and stereoselectivity of the products were confirmed by ^{1}H NMR and ^{13}C NMR analysis (see Supplementary Material).

In cases of mixture of stereoisomers, considering they have the same rf values, they were isolated as a mixture.

3.4. NMR Spectroscopic Data

Spectral data were in agreement with those reported in the literature, as follows.

Styryl(p-tolyl)sulfane [25] (**3a**)*:* Yield: 97%. (E/Z): 82/18. ^{1}H NMR (200 MHz, $CDCl_3$): δ = 7.54–7.06 (m, 9H); 6.85 (d, *J* = 15.5 Hz, 0.82 × 1H); 6.63 (d, *J* = 15.5 Hz, 0.82 × 1H); 6.54 (d, *J* = 10.8 Hz, 0.18 × 1H); 6.44 (d, *J* = 10.8 Hz, 0.18 × 1H); 2.34 (s, 0.82 × 3H); 2.30 (s, 0.18 × 3H) ppm. ^{13}C NMR (75 MHz, $CDCl_3$): δ = 137.5, 136.7, 132.8, 130.7, 130.6, 130.1, 130.0, 128.9, 128.8, 128.4, 127.5, 127.2, 127.1, 126.6, 126.1, 124.6, 21.2.
Phenyl(styryl)sulfane [25] (**3b**)*:* Yield: 82%. (E/Z): 67/33. ^{1}H NMR (300 MHz, $CDCl_3$): δ = 7.46 −7.14 (m, 10H); 6.80 (d, *J* = 15.5 Hz, 0.67 × 1H); 6.64 (d, *J* = 15.5 Hz, 0.67 × 1H); 6.50 (d, *J* = 10.8 Hz, 0.33 × 1H); 6.41 (d, *J* = 10.8 Hz, 0.33 × 1H) ppm. ^{13}C NMR (75 MHz, $CDCl_3$): δ = 136.6, 136.3, 135.3, 131.8, 130.1, 129.9, 129.2, 128.8, 128.7, 128.4, 127.6, 127.3, 127.2, 127.0, 126.1, 123.4 ppm.
(E)-(4-chlorophenyl)(styryl)sulfane [47] (**3c**)*:* Yield: 76%. (E/Z): 100/0. ^{1}H NMR (300 MHz, $CDCl_3$): δ = 7.33–7.24 (m, 9H); 6.82 (d, *J* = 15.4 Hz, 1H), 6.73 (d, *J* = 15.4 Hz, 1H). ^{13}C NMR (75 MHz, $CDCl_3$): δ = 136.3, 133.9, 133.0, 132.8, 131.0, 129.3, 128.7, 127.8, 126.1, 122.5 ppm.
(4-bromophenyl)(styryl)sulfane [17] (**3d**)*:* Yield: 65%. (E/Z): 70/30. ^{1}H NMR (300 MHz, $CDCl_3$): δ = 7.56–7.24 (m, 9H); 6.75 (d, *J* = 15.4 Hz, 0.70 × 1H); 6.82 (d, *J* = 15.4 × 2H); 6.63 (d, *J* = 10.6 Hz, 0.30 × 1H); 6.41 (d, *J* = 10.6 Hz, 0.30 × 1H) ppm. ^{13}C NMR (75MHz, $CDCl_3$):

δ =136.3, 134.6, 133.0, 132.8, 132.2, 131.4, 131.1, 129.0, 128.7, 128.4, 128.2, 127.9, 127.4, 126.3, 126.1, 124.9, 122.2, 120.9 ppm.
Naphthalen-2-yl(styryl)sulfane [48] (**3e**)*:* Yield: 81%. (E/Z): 32/68. ^{1}H NMR (300 MHz, $CDCl_3$): δ = 7.87–7.11 (m, 12H); 6.87 (d, *J* = 15.3 Hz, 0.32 × 1H); 6.69 (d, *J* = 15.3 Hz, 0.32 × 1H); 6.55 (d, J = 10.5 Hz, 0.68 × 1H); 6.49 (d, *J* = 10.5 Hz, 0.68 × 1H) ppm. ^{13}C NMR (75 MHz, $CDCl_3$): δ = 136.5, 133.7, 133.6, 132.3, 132.2, 129.0, 128.9, 128.8, 128.5, 128.4, 128.2, 127.8, 127.7, 127.6, 127.5, 127.4, 127.3, 126.8, 126.6, 126.3, 126.1, 125.8, 125.7, 123.2 ppm.
Cyclohexyl(styryl)sulfane [25] (**3f**)*:* Yield: 73%. (E/Z): 10/90. ^{1}H NMR (300 MHz, $CDCl_3$) δ = 7.41 (d, *J* = 7.20 Hz, 2H); 7.30–7.10 (m, 3H); 6.69 (d, *J* = 15.6 Hz, 0.10 × 1H); 6.50 (d, *J* = 15.6 Hz, 0.10 × 1H); 6.36 (d, *J* = 10.8 Hz, 0.90 × 1H); 6.26 (d, *J* = 10.8 Hz, 0.90 × 1H); 2.87–2.77 (m, 1H); 2.02–1.31 (m, 10H) ppm. ^{13}C NMR (75 MHz, $CDCl_3$) δ = 137.1, 128.6, 128.2, 126.5, 125.9, 125.0, 47.8, 33.7, 29.7, 26.0, 25.6 ppm.
Propyl(styryl)sulfane [30] (**3g**)*:* Yield: 45%. (E/Z): 17/83. ^{1}H NMR (300 MHz, $CDCl_3$) δ = 7.48 (d, *J* = 6.20 Hz, 2H); 7.36–7.16 (m, 3H); 6.71 (d, *J* = 15.6 Hz, 0.17 × 1H); 6.50 (d, *J* = 15.6 Hz, 0.17 × 1H); 6.41 (d, *J* = 10.9 Hz, 0.83 × 1H); 6.23 (d, *J* = 10.9 Hz, 0.83 × 1H); 2.75 (t, *J* = 7.2 Hz, 2H); 1.77–1.65 (m, 2H); 1.02 (t, *J* = 7.2 Hz, 3H) ppm. ^{13}C NMR (75 MHz, $CDCl_3$) δ = 137.1, 128.6, 128.2, 127.7, 126.8, 126.6, 125.5, 125.4, 125.3, 37.9, 34.7, 23.6, 22.9, 13.4, 13.2 ppm.
Butyl(styryl)sulfane [47] (**3h**)*:* Yield: 40%. (E/Z): 12/88. ^{1}H NMR (300 MHz, $CDCl_3$) δ = 7.47 (d, *J* = 6.99 Hz, 2H); 7.36–7.16 (m, 3H); 6.71 (d, *J* = 15.6 Hz, 0.12 × 1H); 6.45 (d, *J* = 15.6 Hz, 0.12 × 1H); 6.41 (d, *J* = 10.9 Hz, 0.88 × 1H); 6.23 (d, *J* = 10.9 Hz, 0.88 × 1H); 2.77 (t, *J* = 7.5 Hz, 2H), 1.66 (quint, *J* = 7.5 Hz, 2H), 1.49–1,37 (m, 2H), 0.92 (t, *J* = 7.5 Hz, 3H) ppm. ^{13}C NMR (75 MHz, $CDCl_3$) δ = 137.1, 128.6, 128.2, 127.7, 126.5, 125.3, 35.6, 32.3, 21.7, 13.6 ppm.
(Z)-3-(2-(p-tolylthio)vinyl)thiophene [49] (**3i**)*:* Yield: 93%. (E/Z): 0/100. ^{1}H NMR (300 MHz, $CDCl_3$): δ = 7.49–7.47 (m, 1H); 7.37 (d, *J* = 8.2 Hz, 2H); 7.30–7.29 (m, 2H); 7.15 (d, *J* = 8.2 Hz, 2H); 6.56 (d, *J* = 10.5 Hz, 1H); 6.37 (d, *J* = 10.5 Hz, 1H); 2.34 (s, 3H) ppm. ^{13}C NMR (75 MHz, $CDCl_3$): δ = 137.9, 137.4, 132.3, 130.5, 130.0, 128.6, 125.7, 125.1, 123.7, 120.9, 21.1 ppm.
(Z)-3-(2-((4-bromophenyl)thio)vinyl)thiophene (**3j**)*:* Yield: 82%. (E/Z): 30/70. ^{1}H NMR (300 MHz, $CDCl_3$): δ = 7.48–7.43 (m, 3H); 7.32–7.7.26 (m, 4H); 6.80 (d, *J* = 15.3 Hz, 0.30 × 1H); 6.66 (d, *J* = 10.5 Hz, 0.70 × 1H); 6.64 (d, *J* = 15.3 Hz, 0.30 × 1H); 6.34 (d, *J* = 10.5 Hz, 0.70 × 1H) ppm. ^{13}C NMR (75 MHz, $CDCl_3$): δ = 138.8, 137.7, 135.2, 134.9, 132.4, 132.3, 131.5, 131.1, 128.6, 128.2, 126.6, 125.4, 124.8, 124.3, 123.5, 122.8, 127.4, 121.7, 121.3, 120.9 ppm.

4. Conclusions

We developed an alternate, eco-friendly, robust, safe, and scalable method for the synthesis of vinyl sulfides via the hydrothiolation of alkynes with thiols using iron-borophosphate glass as a catalyst. In most cases, this new regioselective procedure affords the desired products in good yields. The features of this iron-glass-catalyzed reaction include: (1) ease of preparation; (2) simplicity, non-toxicity, and safety; (3) low catalyst loading; (4) atom economy; (5) solvent-free approach; (6) inexpensiveness; (7) gram scalability; (8) catalyst recyclability; and (9) applicability to structurally diverse substrates. These features render it an environmentally friendly alternative for synthesizing vinyl sulfides. Further applications of iron-borophosphate glass as catalyst in the thiolation of organic structures are in progress in our group.

Supplementary Materials: The following supporting information can be downloaded at https://www.mdpi.com/article/10.3390/catal13071127/s1. Figure S1: Deconvolution spectra of glasses in the region between 800 and 1350 cm^{-1} with (A) 0% Al_2O_3 and 0% Fe_2O_3, (B) 10% Al_2O_3 and 0% Fe_2O_3, and (C) 10% Al_2O_3, 6% Fe_2O_3, and (D) full Raman spectra of the glass-based catalyst (i) after and (ii) before reaction. NMR spectroscopic data for all compounds **3a–3j**. ^{1}H and ^{13}C NMR spectra for all compounds **3a–3j**.

Author Contributions: Conceptualization, R.S., S.S. and G.V.B.; synthesis, spectral analysis, characterizations, and reagents/materials, N.C., E.A.T., I.J.A.G., M.J.A.d.S., F.M., M.G. and J.R., catalyst synthesis and characterizations, J.F.F. and R.S.; organic synthesis, N.C., E.A.T., I.J.A.G. and M.J.A.d.S.; writing—original draft, J.R., R.S., S.S. and G.V.B.; writing—review and editing, J.R., R.S., S.S. and

G.V.B.; writing of the paper, J.R., R.S., S.S. and G.V.B. All authors have read and agreed to the published version of the manuscript.

Funding: This research received no external funding.

Data Availability Statement: The data used to support the findings of this study are included in the article. In addition, the Supplementary Materials include the spectral data of the compounds.

Acknowledgments: We gratefully acknowledge CAPES (001) and CNPq for financial support. G.V.B. acknowledges CNPq for funding (429831/2018-8). R.S. would like to acknowledge CNPq for funding (422774/2018-9). JR and SS are grateful to CNPq for funding (315399/2020-1, 422645/2021-4, 309975/2022-0, and 403210/2021-6). J.F.F. acknowledges CNPq (430470/2018-5) and FAPDF (193.001.757/2017), for financial support.

Conflicts of Interest: The authors declare no conflict of interest.

References

1. Brow, R.K. Nature of Alumina in Phosphate Glass: I, Properties of Sodium Aluminophosphate Glass. *J. Am. Ceram. Soc.* **1993**, *76*, 913–918. [CrossRef]
2. Hoppe, U. A structural model for phosphate glasses. *J. Non-Cryst. Solids* **1996**, *195*, 138–147. [CrossRef]
3. Tupberg, C.; Chandet, N.; Wattanavichan, K.; Randorn, C. Catalytic and antibacterial activities of novel colored zinc borophosphate glasses. *RSC Adv.* **2016**, *6*, 79602–79611. [CrossRef]
4. Rafique, J.; Saba, S.; Frizon, T.E.A.; Braga, A.L. Fe_3O_4 Nanoparticles: A Robust and Magnetically Recoverable Catalyst for Direct C-H Bond Selenylation and Sulfenylation of Benzothiazoles. *ChemistrySelect* **2018**, *3*, 328–334. [CrossRef]
5. Mojtahedi, M.M.; Abaee, M.S.; Rajabi, A.; Mahmoodi, P.; Bagherpoor, S. Recyclable superparamagnetic Fe_3O_4 nanoparticles for efficient catalysis of thiolysis of epoxides. *J. Mol. Catal. A Chem.* **2012**, *361–362*, 68–71. [CrossRef]
6. Godoi, M.; Liz, D.G.; Ricardo, E.W.; Rocha, M.S.T.; Azeredo, J.B.; Braga, A.L. Magnetite (Fe_3O_4) nanoparticles: An efficient and recoverable catalyst for the synthesis of alkynyl chalcogenides (selenides and tellurides) from terminal acetylenes and diorganyl dichalcogenides. *Tetrahedron* **2014**, *70*, 3349–3354. [CrossRef]
7. Kassaee, M.Z.; Motamedi, E.; Movassagh, B.; Poursadeghi, S. Iron-Catalyzed Formation of C–Se and C–Te Bonds through Cross Coupling of Aryl Halides with Se(0) and Te(0)/Nano-Fe_3O_4@GO. *Synthesis* **2013**, *45*, 2337–2342. [CrossRef]
8. Palomba, M.; Bagnoli, L.; Marini, F.; Santi, C.; Sancineto, L. Recent advances in the chemistry of vinylchalcogenides. *Phosphorus Sulfur Silicon Relat. Elem.* **2016**, *191*, 235–244. [CrossRef]
9. Beletskaya, I.P.; Ananikov, V.P. Transition-Metal-Catalyzed C-S, C-Se, and C-Te Bond Formation via Cross-Coupling and Atom-Economic Addition Reactions. *Chem. Rev.* **2011**, *11*, 1596–1636. [CrossRef]
10. Pearson, W.H.; Lee, I.Y.; Mi, Y.; Stoy, P. Total Synthesis of the Kopsia Lapidilecta Alkaloid (±)-Lapidilectine B. *J. Org. Chem.* **2013**, *69*, 9109–9122. [CrossRef]
11. Reddy, V.P.; Swapna, K.; Kumar, A.V.; Rao, K.R. Recyclable Nano Copper Oxide Catalyzed Stereoselective Synthesis of Vinyl Sulfides under Ligand-Free Conditions. *Synlett* **2009**, *17*, 2783–2788. [CrossRef]
12. Kundu, D.; Chatterjee, T.; Ranu, B.C. Magnetically Separable $CuFe_2O_4$ Nanoparticles Catalyzed Ligand-Free C-S Coupling in Water: Access to (E)- and (Z)- Styrenyl- Heteroaryl and Sterically Hindered Aryl Sulfides. *Adv. Synth. Cat.* **2013**, *355*, 2285–2296. [CrossRef]
13. Gonçalves, L.C.C.; Lima, D.B.; Borba, P.M.Y.; Perin, G.; Alves, D.; Jacob, R.G.; Lenardao, E.J. Glycerol/CuI/Zn as a recyclable catalytic system for synthesis of vinyl sulfides and tellurides. *Tetrahedron Lett.* **2013**, *54*, 3475–3480. [CrossRef]
14. Rodygin, K.S.; Gyrdymova, Y.V.; Zarubaev, V.V. Synthesis of vinyl thioethers and bis-thioethenes from calcium carbide and disulfides. *Mendeleev Commun.* **2017**, *27*, 476–478. [CrossRef]
15. Palacios, L.; Giuseppe, A.D.; Artigas, M.J.; Polo, V.; Lahoz, F.J.; Castarlenas, R.; Pérez-Torrente, J.; Oro, L.A. Mechanistic insight into the pyridine enhanced α-selectivity in alkyne hydrothiolation catalysed by quinolinolate-rhodium(I)-N-heterocyclic carbine complexes. *Catal. Sci. Technol.* **2016**, *6*, 8548–8561. [CrossRef]
16. Dondoni, A.; Marra, A. Metal-Catalyzed and Metal-Free Alkyne Hydrothiolation: Synthetic Aspects and Application Trends. *Eur. J. Org. Chem.* **2014**, *2014*, 3955–3969. [CrossRef]
17. Chu, S.; Chung, J.; Park, J.E.; Chung, Y.K. Hydrothiolation of Alkenes and Alkynes Catalyzed by 3,4-Dimethyl-5-vinylthiazolium iodide and Poly (3,4-dimethyl-5-vinylthiazolium) iodide. *ChemCatChem* **2016**, *8*, 2476–2481.
18. Silva, M.S.; Lara, R.G.; Marczewski, J.M.; Jacob, R.G.; Lenardão, E.J.; Perin, G. Synthesis of vinyl sulfides via hydrothiolation of alkynes using Al_2O_3/KF under solvent-free conditions. *Tetrahedron Lett.* **2008**, *49*, 1927–1930. [CrossRef]
19. Rosa, C.H.; Peixoto, M.L.B.; Rosa, G.R.; Godoi, B.; Galetto, F.Z.; D'Oca, M.G.M.; Godoi, M. Sulfamic acid: An efficient and recyclable catalyst for the regioselective hydrothiolation of terminal alkenes and alkynes with thiols. *Tetrahedron Lett.* **2017**, *58*, 3777–3781. [CrossRef]
20. Kondoh, A.; Takami, K.; Yorimitsu, H.; Oshima, K. Stereoselective Hydrothiolation of Alkynes Catalyzed by Cesium Base: Facile Access to (Z)-1-Alkenyl Sulfides. *J. Org. Chem.* **2005**, *70*, 6468–6473. [CrossRef] [PubMed]

21. Liao, Y.; Chen, S.; Jiang, P.; Qi, H.; Deng, G.-J. Stereoselective Formation of Z- or E-Vinyl Thioethers from Arylthiols and Acetylenes under Transition-Metal-Free Condition. *Eur. J. Org. Chem.* **2013**, *2013*, 6878–6885. [CrossRef]
22. Godoi, M.; Leitemberger, A.; Böhs, L.M.C.; Silveira, M.V.; Rafique, J.; D'Oca, M.G.M. Rice straw ash extract, an efficient solvent for regioselective hydrothiolation of alkynes. *Environ. Chem. Lett.* **2019**, *17*, 1441–1446. [CrossRef]
23. Silveira, M.V.; Zandoná, G.; Leitemberger, V.; Böhs, L.M.C.; Lopes, T.J.; Martins, M.L.; Godoi, M. Water Extract of Rice Straw Ash: Experimental Design and Evaluation of Their Activity in the Hydrothiolation Reaction. *Waste Biomass Valorization* **2021**, *12*, 5041–5050. [CrossRef]
24. Corma, A.; González-Arellano, C.; Iglesias, M.; Sánchez, F. Efficient synthesis of vinyl and alkyl sulfides via hydrothiolation of alkynes and electron-deficient olefins using soluble and heterogenized gold complexes catalysts. *Appl. Catal. A Gen.* **2010**, *375*, 49–54. [CrossRef]
25. Riduan, S.N.; Ying, J.Y.; Zhang, Y. Carbon Dioxide Mediated Stereoselective Copper-Catalyzed Reductive Coupling of Alkynes and Thiols. *Org. Lett.* **2012**, *14*, 1780–1783. [CrossRef] [PubMed]
26. Malyshev, D.A.; Scott, N.M.; Marion, N.; Stevens, E.D.; Ananikov, V.P.; Beletskaya, I.P.; Nolan, S.P. Homogeneous Nickel Catalysts for the Selective Transfer of a Single Arylthio Group in the Catalytic Hydrothiolation of Alkynes. *Organometallics* **2006**, *25*, 4462–4470. [CrossRef]
27. Yang, Y.; Rioux, R.M. Highly stereoselective anti-Markovnikov hydrothiolation of alkynes and electron-deficient alkenes by a supported Cu-NHC complex. *Green Chem.* **2014**, *16*, 3916–3925. [CrossRef]
28. Trostyanskaya, I.G.; Beletskaya, I.P. Regio- and Stereoselective Copper-Catalyzed Addition of Aromatic and Aliphatic Thiols to Terminal and Internal Nonactivated Alkynes. *Synlett* **2012**, *23*, 535–540.
29. Rocha, M.S.T.; Rafique, J.; Saba, S.; Azeredo, J.B.; Back, D.; Godoi, M.; Braga, A.L. Regioselective Hydrothiolation of Terminal Acetylene catalyzed by Magnetite (Fe_3O_4) Nanoparticles. *Synth. Comm.* **2017**, *47*, 291–298. [CrossRef]
30. Sarma, R.; Rajesh, N.; Prajapati, D. Indium(III) catalysed substrate selective hydrothiolation of terminal alkynes. *Chem. Comm.* **2012**, *48*, 4014–4016. [CrossRef]
31. Zhao, H.; Peng, J.; Cai, M. Heterogeneous Hydrothiolation of Alkynes with Thiols Catalyzed by Diphosphino-Functionalized MCM-41 Anchored Rhodium Complex. *Catal. Lett.* **2012**, *142*, 138–142. [CrossRef]
32. Modem, S.; Kankala, S.; Balaboina, R.; Thirukovela, N.S.; Jonnalagadda, S.B.; Vadde, R.; Vasam, C.S. Decarbonylation of Salicylaldehyde Activated by p-Cymene Ruthenium(II) Dimer: Implication for Catalytic Alkyne Hydrothiolation. *Eur. J. Org. Chem.* **2016**, *2016*, 4635–4642. [CrossRef]
33. Peterle, M.M.; Scheide, M.R.; Silva, L.T.; Saba, S.; Rafique, J.; Braga, A.L. Copper-Catalyzed Three-Component Reaction of Oxadiazoles, Elemental Se/S and Aryl Iodides: Synthesis of Chalcogenyl (Se/S)-Oxadiazoles. *ChemistrySelect* **2018**, *3*, 13191–13196. [CrossRef]
34. Maragoni, R.; Carvalho, R.E.; Macahado, M.V.; dos Santos, V.B.; Saba, S.; Botteselle, G.V.; Rafique, J. Layered Copper Hydroxide Salts as Catalyst for the "Click" Reaction and Their Application in Methyl Orange Photocatalytic Discoloration. *Catalysts* **2023**, *13*, 426. [CrossRef]
35. Saba, S.; Dos Santos, C.R.; Zavarise, B.R.; Naujorks, A.A.S.; Franco, M.S.; Schneider, A.R.; Scheide, M.R.; Affeldt, R.F.; Rafique, J.; Braga, A.L. Photoinduced, Direct C(sp^2)−H Bond Azo Coupling of Imidazoheteroarenes and Imidazoanilines with Aryl Diazonium Salts Catalyzed by Eosin Y. *Eur. J. Chem.* **2020**, *26*, 4461–4466. [CrossRef] [PubMed]
36. Franco, M.S.; Saba, S.; Rafique, J.; Braga, A.L. KIO_4-mediated Selective Hydroxymethylation/Methylenation of Imidazo-Heteroarenes: A Greener Approach. *Angew. Chem. Int. Ed.* **2021**, *60*, 18454–18460. [CrossRef]
37. Doerner, C.V.; Scheide, M.R.; Nicoleti, C.R.; Durigon, D.C.; Idiarte, V.D.; Sousa, M.J.A.; Mendes, S.R.; Saba, S.; Neto, J.S.S.; Martins, G.M.; et al. Versatile Electrochemical Synthesis of Selenylbenzo[*b*]Furan Derivatives Through the Cyclization of 2-Alkynylphenols. *Front. Chem.* **2022**, *20*, 880099. [CrossRef]
38. Locatelli, P.P.P.; Gurtat, M.; Lenz, G.F.; Marroquin, J.F.R.; Felix, J.F.; Schneider, R.; Borba, C.E. Simple borophosphate glasses for on-demand growth of self-supported copper nanoparticles in the reduction of 4-nitrophenol. *J. Hazard Mater.* **2021**, *15*, 125801. [CrossRef]
39. Doerner, C.V.; Neto, J.S.S.; Cabreira, C.R.; Saba, S.; Sandjo, L.P.; Rafique, J.; Braga, A.L.; de Assis, F.R. Synthesis of 3-selanyl-isoflavones from 2-hydroxyphenyl enaminones using trichloroisocyanuric acid (TCCA): A sustainable approach. *New J. Chem.* **2023**, *47*, 5598–5602. [CrossRef]
40. Tavares, C.J.; Willig, J.C.M.; Manarin, F.; Lenz, G.F.; Felix, J.F.; Botteselle, G.V.; Schneider, R. Copper nanoparticles growth on the borophosphate glass surface by bottom-up approach: A catalyst for click reactions. *J. Non-Cryst. Solids* **2023**, *610*, 122303. [CrossRef]
41. Velli, L.L.; Varsamis, C.P.E.; Kamitsos, E.I.; Möncke, D.; Ehrt, D. Structural investigation of metaphosphate glasses. *Phys. Chem. Glasses* **2005**, *46*, 178–181.
42. Ducel, J.F.; Videau, J.J.; Couzi, M. Structural study of borophosphate glasses by raman and infrared spectroscopy. *Phys. Chem. Glas.* **1993**, *34*, 212–218.
43. Anastasopoulou, M.; Vasilopoulos, K.C.; Anagnostopoulos, D.; Koutselas, I.; Papayannis, D.K.; Karakassides, M.A. Structural and theoretical study of strontium borophosphate glasses using Raman spectroscopy and ab initio molecular orbital method. *J. Phys. Chem. B* **2017**, *121*, 4610–4619. [CrossRef] [PubMed]

44. Moguš-Milanković, A.; Gajović, A.; Šantić, A.; Day, D. Structure of sodium phosphate glasses containing Al_2O_3 and/or Fe_2O_3. *J. Non-Cryst. Solids* **2001**, *289*, 204–213. [CrossRef]
45. Scagliotti, M.; Villa, M.; Chiodelli, G. Short range order in the network of the borophosphate glasses: Raman results. *J. Non Cryst. Solids* **1987**, *93*, 350–360. [CrossRef]
46. Hudgens, J.J.; Brow, R.K.; Tallant, D.R.; Martin, S.W. Raman Spectroscopy Study of the Structure of Lithium and Sodium Ultraphosphate Glasses. *J. Non-Cryst. Solids* **1998**, *223*, 21–31. [CrossRef]
47. Lin, Y.-M.; Lu, G.-P.; Wang, G.-X.; Yi, W.-B. Acid/Phosphide-Induced Radical Route to Alkyl and Alkenyl Sulfides and Phosphonothioates from Sodium Arylsulfinates in Water. *J. Org. Chem.* **2017**, *82*, 382–389. [CrossRef]
48. Ranjit, S.; Duan, Z.; Zhang, P.; Liu, X. Synthesis of Vinyl Sulfides by Copper-Catalyzed Decarboxylative C−S Cross-Coupling. *Org. Lett.* **2010**, *12*, 4134–4136. [CrossRef]
49. Patel, M.; Saunthwal, R.K.; Dhaked, D.K.; Bharatam, P.V.; Verma, A.K. Nucleophilic Addition versus SNAr Study: Chemo-, Regio- and Stereoselective Hydrothiolation of Haloaryl Alkynes over S-Arylation of Aryl Halides. *Asian J. Org. Chem.* **2015**, *4*, 894–898. [CrossRef]